Ultrafast Acoustic Gating of Photocurrent in Nanodevices with Quantum Wells

A. V. Akimov,[1,*] D. Moss,[1] B. A. Glavin,[2] O. Makarovsky,[1]
R. P. Campion,[1] C. T. Foxon,[1] L. Eaves,[1] and A. J. Kent[1]

[1]*School of Physics and Astronomy, University of Nottingham, University Park, Nottingham NG7 2RD, UK*
[2]*Institute of Semiconductor Physics, National Academy of Sciences, Kiev 03028, Ukraine*
(Received April 18, 2010)

Picosecond acoustic wave packets are used to control the photocurrent excited by a femtosecond optical pulse in multilayer GaAs-based devices containing a quantum well. The change in photocurrent arises from the strain-induced shift of the quantum-well excitonic resonance due to the deformation potential of electron–phonon coupling.

PACS numbers: 72.80.Ey, 72.50. +b, 85.30.Mn

I. INTRODUCTION

It is attractive to apply the experimental methods of picosecond acoustics to control electronic-device properties on ultrafast timescales. Acoustic techniques at GHz frequencies have proved to be a powerful tool for controlling the optical and electronic properties of semiconductor nanostructure devices [1, 2]. The use of picosecond acoustics could increase the frequency to the THz range. Methods developed during the last two decades provide for the generation and detection of picosecond strain pulses and wave packets [3, 4], acoustic solitons [5], THz harmonic elastic oscillations in superlattices [6, 7], and phonon microcavities [8]. The effects of picosecond strain pulses on the optical reflectivity and photoluminescence spectra of semiconductor nanostructures have demonstrated the feasibility of ultrafast control of the optical properties by means of picosecond acoustic techniques [9]. However, the control, on a picosecond time scale, of the electrical transport properties of a device using acoustic waves is still a challenge.

Recently, using the picosecond acoustic technique, we have realized the ultrafast gating of a photocurrent in a p-i-n diode [10]. Here, the picosecond strain and optical pulses act simultaneously upon the quantum well (QW) embedded in the intrinsic layer of a p-i-n tunneling diode. In the present paper, we present the bias-voltage dependency and the excitation-wavelength dependency of a photocurrent signal obtained in ultrafast gating experiments.

The idea of the experiments is based on the strong sensitivity of the electron–hole (i.e., exciton) excitation energy, E_0, in the QW to the applied strain ε, known as the piezospectroscopic effect [11]. The experimental idea for a p-i-n tunneling device is illustrated in Fig. 1. By using the strain pulse $\varepsilon(t)$ to modulate E_0, we are able to tune or detune

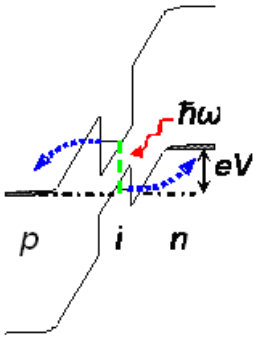

FIG. 1: The band diagram of p-i-n diode with a QW when the reverse bias is applied. The dashed vertical and curved lines show optical and tunneling transitions in the QW.

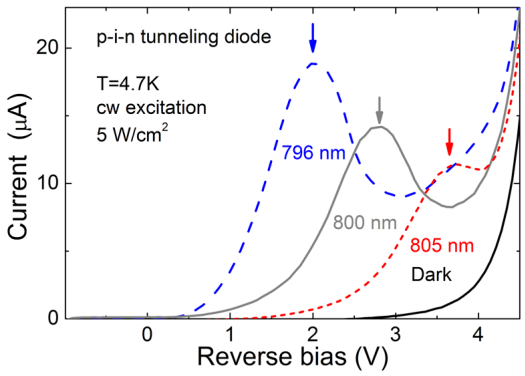

FIG. 2: I–V curves measured in the dark and under illumination for different wavelengths of CW optical excitation.

the exciton resonance with the energy $\hbar\omega$ of the incident photons from a laser probe beam. The optical absorption, and hence the number of photoexcited carriers in the QW, depends on $(E_0 - \hbar\omega)$ and thus follows $\varepsilon(t)$. Then the photocurrent, excited by a short optical pulse simultaneously with the strain pulse, is related directly to $\varepsilon(t)$ in the QW. Thus, the strain pulse $\varepsilon(t)$ plays the role of an ultrafast gate controlling the photocurrent in a device with a QW.

II. EXPERIMENT

GaAs/AlGaAs p-i-n tunneling device

The p-i-n device used in the experiments was grown by molecular beam epitaxy on a semi-insulating GaAs substrate of a thickness $l = 375$ μm. The active structure consists of a single 7.5-nm-thick undoped GaAs QW confined between two 100-nm-wide undoped $Al_{0.3}Ga_{0.7}As$ layers. The n and p contacts were Si-doped and C-doped (both 10^{18} cm^{-3}) 200-nm-wide layers of $Al_{0.3}Ga_{0.7}As$, respectively. The structure was processed into mesas of diameter 400 μm with ring-shaped electrical contacts to allow optical access. A schematic band diagram of the p-i-n RTD under reverse bias is shown in Fig. 1.

The experiments were performed in an optical cryostat at $T = 4.7$ K. To characterize the device and obtain values of E_0 as a function of reverse bias, V, the current–voltage (I–V) characteristics, shown in Fig. 2, were measured in the dark and under CW photoexcitation at different wavelengths. The peaks in the photocurrent, indicated by the vertical arrows in Fig. 2, correspond to the condition when the photon energy $\hbar\omega \approx E_0$ [12]. The applied reverse bias, V, reduces the value of E_0 in the QW due to the quantum-confined Stark effect [13], and hence, the bias value of the peak in the I–V curve increases with the excitation

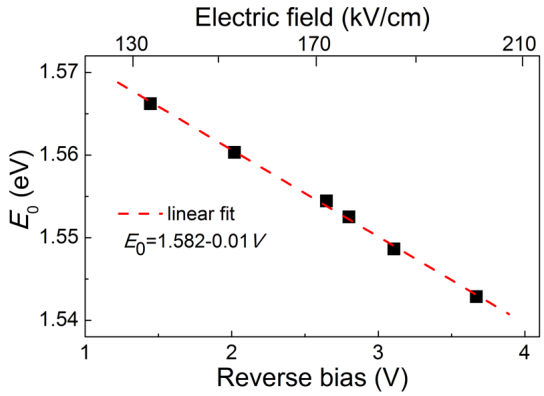

FIG. 3: Bias dependence of the exciton resonance energy E_0 of the QW, obtained from the position of peaks in the I–V curves for various excitation wavelengths. The upper horizontal scale shows the electric field in the QW calculated from the experimental values of E_0.

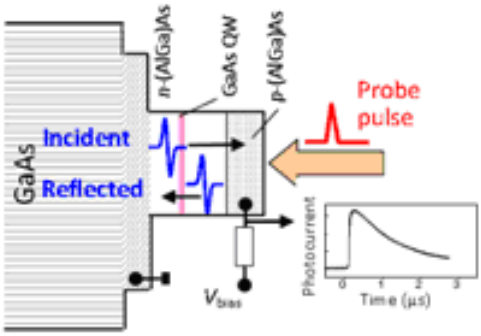

FIG. 4: The schematic diagram of ultrafast probing of the photocurrent changes in the p-i-n structure, showing the bipolar strain pulses arriving at the QW due to the initial strain pulse and the pulse reflected from the top surface of the device.

wavelength. The measured dependence of E_0 on V obtained from the I–V curves is shown in Fig. 3.

In the ultrafast experiments, the picosecond strain pulses were generated in a 100-nm -thick Al-film deposited on the polished side of the GaAs substrate opposite to the p-i-n structure. The film was excited by $\sim$ 150-fs optical pump pulses with a variable wavelength in the range of 700 to 1000 nm and repetition rate of 83 MHz. The laser beam was focused to a spot with a diameter of 100 μm on the surface of the Al film exactly opposite to the optical mesa of the p-i-n structure. Because of the thermoelastic effect, a 10-ps duration bipolar strain pulse $\varepsilon(t, z)$, where z is the coordinate perpendicular to the interface of the substrate with the metal film, was generated in the film. The strain pulse was injected from the Al film into the GaAs substrate and it reached the p-i-n structure after traversing the GaAs substrate in the time $t_0 = l/s_L = 78$ ns, where $s_L = 4.8 \times 10^3$ m/s is the longitudinal (LA) sound velocity in GaAs. The excitation density in the focused pump spot did not exceed 0.1 mJ/cm^2. This corresponds to a strain pulse amplitude of less than 10^{-4}, which is well below the values at which nonlinear elastic effects (i.e., shock waves and acoustic solitons) become important.

The experimental setup for detecting the effect of the strain pulse in the p-i-n structure is shown in Fig. 4. The p-i-n diode was excited by a femtosecond optical probe beam split from the same laser that was used to excite the Al film. The spectrum of the probe pulse was centered at the photon energy $\hbar\omega$ close to E_0 and had a width of 14 meV. The beam was focused to a spot of 50 μm at the center of the optical mesa with an energy density of $\sim$ 1 nJ/cm^2. The probe pulse excited a microsecond-long photocurrent pulse in the device as shown in the frame in Fig. 4. The signal was amplified, and the time-integrated photocurrent signal P was measured as a function of time delay t between the optical pump

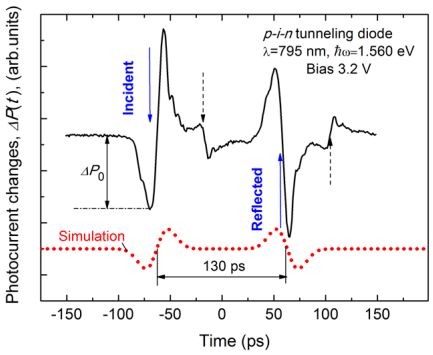

FIG. 5: The temporal trace (solid line) of the photocurrent changes. Solid vertical arrows indicate the arrival of the middle of incident and reflected strain pulses. Dashed vertical arrows show the next echoes generated in an Al film transducer. The dotted line is the simulated temporal trace when the incident and reflected bipolar strain pulses pass through the QW.

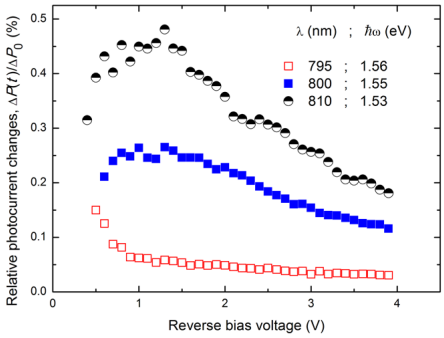

FIG. 6: The dependencies of the relative photocurrent changes amplitude $\Delta P_0/P_0$ on reverse bias voltage measured for three various excitation wavelengths λ. Corresponding photon energies $\hbar\omega$ are also indicated.

and probe pulses. In order to pick out the strain-induced signal $\Delta P(t) = P(t) - P_0$ (P_0 is the signal without a strain pulse), the pump pulse was modulated by an acousto-optical modulator with a frequency of 80 kHz, and a lock-in amplifier was used for the detection of $\Delta P(t)$.

Figure 5 shows the temporal evolution of the strain-induced photocurrent changes $\Delta P(t)$. Ultrafast temporal changes of $\Delta P(t)$ start with a decrease in photocurrent. The analysis given in Ref. [10] (see also sec. III of the present paper) shows that this corresponds to the increase in E_0. In a GaAs QW, this happens if the leading part of the strain pulse $\varepsilon(t)$ is compressive, i.e., $\varepsilon < 0$, as is well known to be the case in picosecond acoustic experiments with optical excitation of a metal film [4, 5]. Next, the tensile part of $\varepsilon(t)$ reaches the QW, and $\Delta P(t)$ increases. This bipolar behavior is repeated in reverse order after a delay of 130 ps due to the passage of a reflected pulse, as explained below.

The trace in Fig. 5 fits well the simulated temporal curve, obtained when only the effect of the strain pulse on the number of photoexcited carriers in the QW is considered, and is shown by the red dotted line in Fig. 5. The spatial length of ~ 200 nm of the strain pulse is much wider than the QW and thus, at each point of time t, the strain $\varepsilon(t)$ in the QW may be considered constant. The $\Delta P(t$ trace consists of two bipolar pulses (shown by vertical solid arrows in Fig. 5), which correspond to the arrival to the QW of incident and reflected strain pulses propagating from the GaAs substrate towards the top surface of the p-i-n structure and back from the surface towards the GaAs substrate, respectively (see the scheme in Fig. 4). The 130-ps difference in the arrival times of the incident and reflected pulses to the QW is the propagation time for longitudinal polarized sound over a

distance of 620 nm from the QW to the surface and back. The incident and reflected pulses have opposite phases due to the phase change at reflection. The value $t = 0$ in Fig. 2(b) is chosen as a time when the center of $\varepsilon(t)$ reaches the surface of the sample. The signal $\Delta P(t)$ consists of additional features (shown by dashed arrows in Fig. 5), which appear in the temporal traces and are known to be due to the reflection of the strain pulse in the 100-nm Al transducer.

The temporal shape $\Delta P(t)$ does not vary with changing bias voltage, V, and the probe-photon energy $\hbar\omega$, but the amplitude ΔP_0 of the signal depends strongly on these values. Figure 6 shows the dependence of the relative changes $\Delta P_0/P_0$ of the photocurrent amplitude. It is seen that $\Delta P_0/P_0$ decreases with an increase in V.

The key result of the experiments with a tunneling p-i-n device is the observation of the pump-probe signal, which follows the temporal evolution of the picosecond strain pulse $\varepsilon(t)$ in the QW. Unambiguous evidence for this is that the incident and reflected pulses are separated by $\Delta t = 130$ ps, which is exactly the propagation time of the pulse from the QW to the surface and back to the QW again. Therefore, when probing by the laser pulse with $\hbar\omega \sim E_0$, any ultrafast strain-induced effects produced when the strain pulse passes through other parts of the device make no significant contribution to the photocurrent.

III. THEORETICAL ANALYSIS

Here, we present the theoretical procedure, which can be used to quantitatively calculate the photocurrent signal induced by acoustic gating effect. For this, it is necessary to know the value of the electric field F in the QW and its dependence on V. This was obtained from calculations of the electron and hole eigenstates in the QW as a function of F, and by comparing this with the measured dependence of E_0 on V presented in Fig. 3. The measured dependence of F on V is almost linear and can be found from the comparison of the upper and lower scales in Fig. 3. Theoretical analysis based on the band diagram, as schematically shown in Fig. 1, gives the effective thickness of the insulator layer in the p-i-n structure: $d_i = (eV + E_g)/F$ (where E_g is the bandgap in the doped AlGaAs contacts). At liquid helium temperatures, the value of d_i increases noticeably with V and is 20–40% larger than the nominal grown thickness (207.5 nm) because of the depletion regions in the (AlGa)As contacts. The relatively low free-carrier density $\sim 10^{17}$ cm^{-3} in the p-contact at $T = 4.7$ K, as estimated from the dependence of F on V is confirmed by capacitance–voltage measurements. which show that the (AlGa)As contacts are partially frozen out at these low temperatures.

Using the dependence of F on V, we estimate the changes in the photocurrent provided by the acoustical gating for various mechanisms of the electron–phonon interaction in the QW. The temporally integrated photocurrent generated by the carriers excited optically in the QW may be written as follows:

$$P = \frac{2eN\tau_{rad}}{\tau_t + \tau_{rad}}, \tag{1}$$

where N is the number of photoexcited electron–hole pairs in the QW; τ_t is the time of carrier tunneling from the QW; and τ_{rad} is the carrier recombination time in the QW. Using the Wentzel-Kramers-Brillouin (WKB) approximation, it is found that for the relevant values of F (see Fig. 3), τ_t ∼1–100 ps, which is much less than τ_{rad} ∼1 ns. Therefore, from Eq. (1), it is found that the major fraction of photoexcited carriers contribute to the photocurrent.

The number of photoexcited electrons and holes is given by

$$N = \int d\omega \frac{I(\omega)}{\hbar\omega} A(\omega), \tag{2}$$

where $I(\omega)$ is the spectral density of the probe optical energy flux and $A(\omega)$ is the QW absorption efficiency. In our ultrafast experiments, $I(\omega)$ can be approximated by a Gaussian, $I(\omega) \sim \exp\left(-\frac{(\omega-\omega_0)^2}{2\Delta\omega^2}\right)$, where the broadening parameter $\Delta\omega \approx 4.9$ meV.

On analyzing the effect of strain on the photocurrent, at first, it is assumed that the kinetic parameters τ_t and τ_{rad} are insensitive to strain. Then, the strain-induced changes of P are governed only by the modification of $A(\omega)$. The strain ε modifies $A(\omega)$ by changing the bandgap in the QW due to the deformation potential, i.e., $A(\omega) = A_0(\omega) - \frac{dA}{d\omega} E_1\varepsilon/\hbar$, where $A_0(\omega)$ is the absorption spectrum at $\varepsilon = 0$ and E_1 is the deformation potential (for GaAs $E_1 \approx -10$ eV). The strain-induced relative changes in the photocurrent can then be written as

$$\frac{\Delta P}{P_0} = -\frac{E_1\varepsilon \int d\omega I(\omega)\frac{dA}{d\omega}}{\hbar \int d\omega I(\omega)A(\omega)}. \tag{3}$$

In addition to the deformation potential, there are other mechanisms that can cause strain-induced changes in $A(\omega)$ [14–16]. Numerical estimates for our device indicate that all these effects are small, typically less than 10% of the contribution from the deformation potential.

The modeling of the spectral shape of $A(\omega)$ can be made from the detailed studies of the optical absorption or photoluminescence excitation spectra. This task lies beyond the scope of the present manuscript, and here, for simplicity, we take $A(\omega)$ as a step occurring at the edge $\omega_{e\text{-}h}$ of the optical transitions between the electron and hole confined states in the QW. Then $A(\omega) = 0$ for $\omega < \omega_{e\text{-}h}$. Such simplified spectral shape does not include the narrow peaks from the exciton transitions [12]. Fig. 7 shows the bias dependences of the sensitivity $\alpha = \frac{\Delta P}{\varepsilon P_0}$ of the detected signal ΔP on ε calculated using Eq. (3). A decrease in $\Delta P_0/P_0$ with an increase in the reverse bias voltage V is observed. The experimentally measured curves (Fig. 6) also show a decrease with an increase in V for $|V| > 1$ V. For more precise quantitative comparison, one should use various spectral shapes of $A(\omega)$. This has been performed in our earlier study where strain pulses with much higher amplitude than in the present study were used [10].

The analysis, based on Eq. (3), assumed that the kinetic parameters τ_t and τ_{rad} are strain-independent. This assumption is justified by the experimental result that shows weak

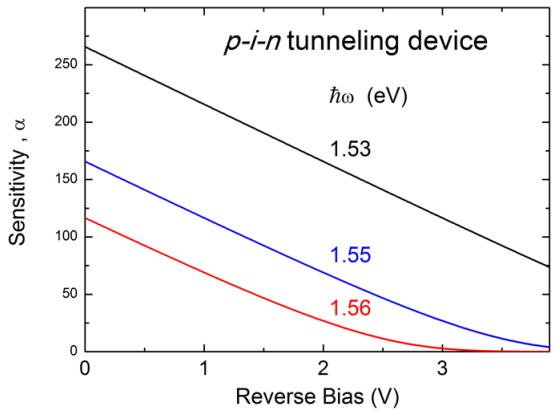

FIG. 7: Calculated dependency of the photocurrent sensitivity α to the strain for three excitation-photon energies. The calculations are performed for the p-i-n structure used in the experiments.

dependence of the temporal shape $\Delta P(t)$ on V. Indeed, any strain-induced changes of τ_t or τ_{rad} should be detected in the time interval that the carriers are present in the QW after the probe pulse. In this case, $\Delta P(t)$ is the result of the time convolution of the strain pulse $\varepsilon(t)$ and the temporal decay of the photoexcited carrier densities in the QW. The estimated values of $\tau_t \sim$ 1–100 ps vary with V over orders of magnitude. Therefore, if τ_t and τ_{rad} were strain-dependant, the temporal shape of $\Delta P(t)$ would be strongly dependent on V, but this is not observed in the experiments.

IV. CONCLUSIONS

We have shown that a picosecond strain pulse can be used to gate, on a picosecond timescale, the photocurrent in a p-i-n diode containing a QW in its intrinsic region. The effects are linked to the QW, while all other regions of the device, such as the barriers and contacts, are not affected by the strain on this time scale. Regardless of the fact that the external circuit is limited to GHz speeds, these experiments demonstrate that ultrafast control of the internal electron processes using strain pulses is possible. The sensitivity to strain is at least one order of magnitude higher than in the traditional pump-probe techniques, where the reflectivity changes due to the elasto-optical effect are measured. This could lead to the development of techniques for clocking devices with THz acoustic waves. The method is not limited to the simple devices with QWs, and it could be extended to quantum-dot nanostructures and various tunneling devices with the strain-sensitive electronic resonances. In planar photocurrent devices, this method can be used for probing buried nanostructures and obtaining the information about the distance of the device location from the surface.

Acknowledgments

We acknowledge financial support from the UK Engineering and Physical Sciences Research Council and the Royal Society.

References

* Electronic address: andrey.akimov@nottingham.ac.uk

[1] M. M. de Lima *et al.*, Phys. Rev. Lett. **97**, 045501 (2006).
[2] M. R. Astley *et al.*, Phys. Rev. Lett. **99**, 156802 (2007).
[3] C. Thomsen *et al.*, Phys. Rev. B **34**, 4129 (1986).
[4] O. B. Wright, Phys. Rev. B **49**, 9985 (1994).
[5] H.-Y. Hao and H. J. Maris, Phys. Rev. B **64**, 064302 (2001).
[6] A. Bartels *et al.*, Phys. Rev. Lett. **82**, 1044 (1999).
[7] C.-K. Sun, J.-C. Liang, and X.-Y. Yu, Phys. Rev. Lett. **84**, 179 (2000).
[8] A. Huynh *et al.*, Phys. Rev. B **78**, 233302 (2008).
[9] A. V. Akimov *et al.*, Phys. Rev. Lett. **97**, 037401 (2006).
[10] D. Moss *et al.*, Phys. Rev. B **80**, 113306 (2009).
[11] E. F. Gross and A. A. Kaplyanskii, Soviet Physics Solid State **2**, 1518 (1961).
[12] S. Schmitt-Rink, D. S. Chelma, and D. A. B. Miller, Adv. Phys., **38**, 89 (1989).
[13] D. A. B. Miller *et al.*, Phys. Rev. B **32**, 1043 (1985).
[14] B. A. Glavin *et al.*, Phys. Rev. B **71**, 081305(R) (2005).
[15] F. T. Vasko and V. V. Mitin, Phys. Rev. B **52**, 1500 (1994).
[16] V. I. Pipa, V. V. Mitin, M. Stroscio, Appl. Phys. Lett. **74**, 1585 (1999).